JOURNAL OF MATERIALS SCIENCE 31 (1996) 5391–5398

Microstructural development of ZnO varistor during reactive liquid phase sintering

E. R. LEITE, M. A. L. NOBRE, E. LONGO
Departamento de Química, Universidade Federal de São Carlos, Caixa Postal 676, 13565–905 São Carlos, SP, Brasil

J. A. VARELA
Instituto de Química, Universidade Estadual Paulista, Caixa Postal 355, 14800–900 Araraquara, SP, Brasil

The microstructural evolution, grain growth and densification for the varistor systems $ZnO–Bi_2O_3$ (ZB), $ZnO–Bi_2O_3–Sb_2O_3$ (ZBS), $ZnO–Bi_2O_3–Sb_2O_3–MnO–Cr_2O_3–CoO$ (ZBSCCM) were studied using constant heating rate sintering, scanning electron microscopy (SEM) and *in situ* phase formation measurement by high temperature X-ray diffraction (HT-XRD). The results showed that the densifying process is controlled by the formation and decomposition of the $Zn_2Bi_3Sb_3O_{14}$ pyrochlore (PY) phase for the ZBS and ZBSCCM systems. The addition of transition metals (ZBSCCM system) alters the formation and decomposition reaction temperatures of the pyrochlore phase and the morphology of the $Zn_7Sb_2O_{12}$ spinel phase. Thus, the spinel grains act as inclusions and decrease the ZnO grain growth rate. Spinel grain growth kinetics in the ZBSCCM system showed an n value of 2.6, and SEM and HT-XRD results indicate two grain growth mechanisms based on coalescence and Ostwald ripening.

1. Introduction

ZnO-based semiconducting ceramic devices show highly non-linear behaviour between voltage and electric current. This non-ohmic characteristic is related to its microstructure [1, 2]. Thus, knowledge of microstructural development, i.e. phase evolution densification and grain growth, is of fundamental importance in controlling the electric properties of ZnO-based varistors.

The evolution of phases in ZnO-based ceramics was extensively studied by Inada [3, 4], and Inada and Matsuoka [5]. In these studies the $ZnO–Sb_2O_3–Bi_2O_3$ (ZBS) ternary system is considered as basic, and responsible for the microstructural and phase formation of the ZnO-based varistors. During the sintering process of the ZBS system, formation of a pyrochlore type phase ($Zn_2Bi_3Sb_3O_{14}$) occurs, that can react with the ZnO rich matrix according to the reaction [3, 4]

$$2Zn_2Bi_3Sb_3O_{14} + 17ZnO \xrightarrow{950–1050\,^{\circ}C} 3Zn_7Sb_2O_{12} + 3Bi_2O_3(l) \quad (1)$$

Additives of CoO, MnO_2 and Cr_2O_3 largely influence Equation 1, altering the reaction temperature promoting the nucleation of a $Zn_7Sb_2O_{12}$ phase at lower temperatures [3]. During slow cooling Equation 1 can be reversed, due to reaction of the spinel phase with liquid Bi_2O_3; as indicated by Equation 2 [3, 4]

$$3Zn_7Sb_2O_{12} + 3Bi_2O_3(l) \xrightarrow[\text{cooling}]{\text{slow}} 2Zn_2Bi_3Sb_3O_{14} + 17ZnO \quad (2)$$

Several works report the densification as well as the grain growth kinetics of Bi_2O_3 and Bi_2O_3, plus Sb_2O_3-doped ZnO [6–9]. The formation of Bi_2O_3-rich eutectic liquid controls the densification and grain growth mechanisms in the $ZnO–Bi_2O_3$ system [6, 7]. Kim *et al.* [9] showed that the $Sb_2O_3:Bi_2O_3$ ratio controls the temperature for liquid formation in the ZBS system. For $Sb_2O_3:Bi_2O_3 < 1$, the eutectic liquid is formed around 750 °C; associated with the $ZnO–Bi_2O_3$ system. For $Sb_2O_3:Bi_2O_3 > 1$, the Bi_2O_3-rich liquid is formed at temperatures around 1000 °C; due to reaction among pyrochlore and ZnO, as described by Equation 1.

Few works study densification and grain growth kinetics of the transition metal doped ZBS system. Asokan *et al.* [10] report that the addition of CoO or MnO_2 prevents Bi_2O_3 evaporation at high sintering temperatures, and that the addition of Cr_2O_3 and NiO can control ZnO grain growth in a system containing Bi_2O_3, Nb_2O_5, Sb_2O_3, CoO and MnO_2. Chen and Shen [11] report that for the system containing ZnO, Bi_2O_3, Cr_2O_3 and Sb_2O_3, the CoO valence can alter the ZnO grain growth kinetics through the control of zinc vacancies, V_{Zn}, concentration due to

0022–2461

substitution of Zn^{2+} by Co^{3+}, according to the equation

$$Co_2O_3 \xrightarrow{ZnO} 2Co^{\bullet}_{Zn} + V''_{Zn} + 3O^{x}_{o} \quad (3)$$

Chen and Shen [11] considered that the Co^{+3} in the ZnO matrix inhibits the effect of bismuth-rich liquid effect during sintering. Both Chen and Shen [11] and Asokan *et al.* [10] considered the direct effect of additives on ZnO grains, but did not mention the probable effect of these additives on phase formation during the sintering process.

This study aims to analyse the microstructural evolution of $ZnO–Bi_2O_3$ (ZB), $ZnO–Bi_2O_3–Sb_2O_3$ (ZBS) and $ZnO–Bi_2O_3–Sb_2O_3–CoO–Cr_2O_3–MnO_2$ (ZBSCCM) systems through the densification, grain growth and phase evolution analyses using a constant heating rate, HT-XRD and on SEM coupled with Energy dispersive spectroscopy (SEM–EDS).

2. Experimental procedure

2.1. Sample preparation

ZnO and oxide additives were ball milled in a polypropylene jar with stabilized zirconia balls using an isopropanol alcohol medium. The raw materials' characteristics are listed in Table I and the chemical compositions of the samples studied are listed in Table II. To study the densification and grain growth the samples were isostatically pressed at 210 MPa, reaching a green density of $3.37 \pm 0.03\,g\,cm^{-3}$ for all considered systems. The samples were then sintered in a dilatometer furnace (model 402 E Netzsch) with a heating rate of 2.5, 5, 7.5 and $10\,^{\circ}C\,min^{-1}$ for temperatures up to 1200 °C and then cooling down with no soaking time, in atmospheric air.

2.2. Microstructural evolution

Mercury porosimetry (Porosimeter model 9320, Micromeritics) and an SEM (model 940 A, Zeiss) with energy disperse microanalysis (EDS) were used to analyse microstructural evolution. For the pore size distribution measurements the samples were sintered in a dilatometer at a constant heating rate of $10\,^{\circ}C\,min^{-1}$ for temperatures ranging from 700 to 900 °C and cooled in atmospheric air. For SEM inspection the samples were polished and chemically attacked by NaOH (1 M) for several minutes. The samples were then carbon covered to avoid electrostatic charging.

The mean grain size, G, of sintered samples was determined by the intercept method considering the following relationship [12]

$$G = 1.56\,L \quad (4)$$

TABLE I Physical and chemical characteristics of oxides used in this study

Oxides	Purity (%)	Surface area ($m^2\,g^{-1}$)	Mean particle size (μm)
ZnO	99.9	5.0	0.21
Bi_2O_3	99.9	0.8	0.84
Sb_2O_3	> 99.0	2.0	0.53
CoO	> 99.0	3.6	0.29
MnO	> 99.0	9.3	0.13
Cr_2O_3	99.9	3.0	0.38

where L is the mean intercept size of the grain boundary from six random lines distributed in the micrograph. Grain sizes were measured in samples sintered at different heating rates up to 1200 °C.

To study grain growth, the general kinetics equation is given by

$$G^n - G_0^n = kt \quad (5)$$

where G is the mean grain size, G_0 is the initial mean grain size, t is time and n is the grain growth kinetic exponent, was adapted for a constant heating rate. Considering that $G \gg G_0$ and that the constant heating rate, α, is given by

$$\alpha = dT/dt \quad (6)$$

where T is the temperature, Equation 5 can be modified to

$$G^n = (K/\alpha)\,(T - T_0) \quad (7)$$

where T_0 is the temperature for $t = 0$. Equation 7 relates grain growth as a function of temperature for a constant heating rate. By plotting $\ln(G)$ versus $\ln(1/\alpha)$ for the same final temperature, the value of n can be determined considering the slope of a straight line. The value of K can also be determined by the intercept of the straight line with the ordinate axis.

2.3. Phase evolution

Aiming to investigate the phase evolution during sintering of ZBS and ZBSCCM systems, samples containing twice the concentration of dopants, as considered in the sintering studies, were prepared (1 mol % Bi_2O_3, MnO_2 and CoO; 0.2 mol % Cr_2O_3; and 2 mol % Sb_2O_3). The samples were analysed in a high temperature XRD camera (model HDK S1, Edmund Buhler), using an XRD with CuK_α radiation and an Ni filter (model D5000, Siemens). Phase evolution was evaluated in the temperature range 600–1100 °C in atmospheric air. The ZBS system was also characterized by simultaneous differential

TABLE II Chemical compositions used in this study

System	ZnO (mol %)	Bi_2O_3 (mol %)	Sb_2O_3 (mol %)	CoO (mol %)	Cr_2O_3 (mol %)	MnO_2 (mol %)
ZB	99.5	0.5	–	–	–	–
ZBS	98.5	0.5	1.0	–	–	–
ZBSCCM	97.4	0.5	1.0	0.5	0.1	0.5

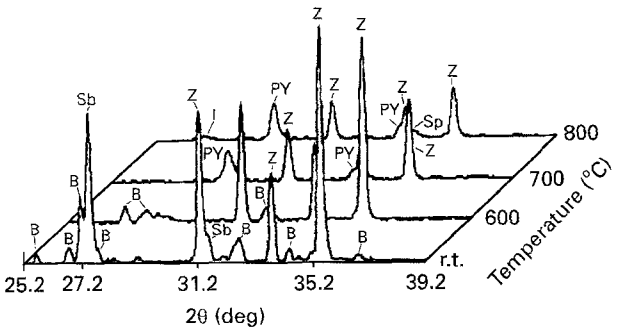

Figure 1 High temperature X-ray diffraction for the ZBS system. r.t., room temperature; B, Bi_2O_3; Sb, Sb_2O_3; Z, ZnO; PY, $Zn_2Bi_3Sb_3O_{14}$; SP, $Zn_7Sb_2O_{12}$; I, $ZnSb_2O_6$.

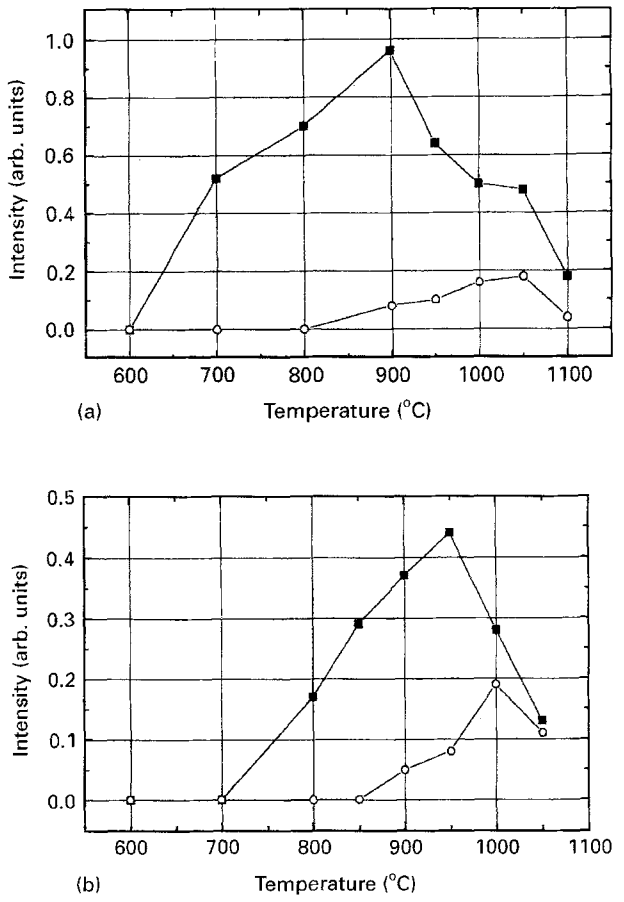

Figure 2 Evolution of phases as function of temperature: (a) for the ZBS system, and (b) for the ZBSCCM system. (—■—) PY, (—○—) SP.

thermal analysis (TGA–DTA model 409 E Netzsch) heating up to 1200 °C, with a heating rate of 10 °C min^{-1} in synthetic air.

3. Results and discussion

3.1. Phase evolution

To analyse the phase evolution with sintering temperature, samples were heated at temperatures ranging from 600 to 800 °C. Fig. 1 shows the XRD patterns for the ZBS system. In this figure, at 600 °C the corresponding peaks of the Sb_2O_3 phase disappear, and between 700 and 800 °C gradual formation of the $Zn_2Bi_3Sb_3O_{14}$ phase (PY) is observed.

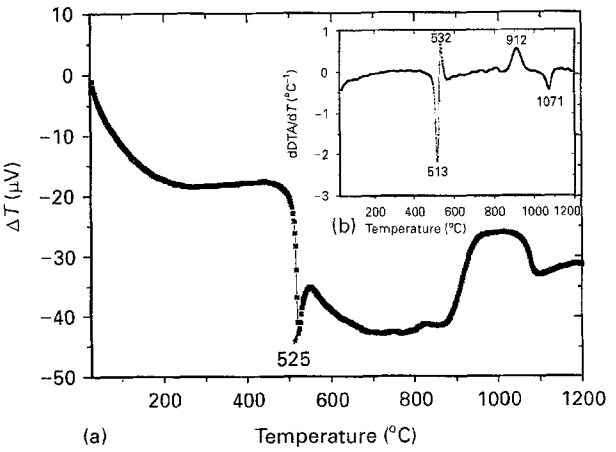

Figure 3 Differential thermal analysis for the ZBS system ($\alpha = 10\,°C\,min^{-1}$): (a) DTA curve; and (b) d(DTA)/dT curve.

Fig. 2 shows the phase evolution with temperature for the ZBS system (Fig. 2a) and for the ZBSCCM system (Fig. 2b) obtained by HT-XRD. In the ZBS system (Fig. 2a), the pyrochlore phase is formed in the 700–900 °C range, and reaction of this phase with ZnO, forming spinel, occurs in the range 900–1100 °C. The spinel phase formed in this temperature range start to decompose at 1050 °C, indicating dissolution of this phase in the formed liquid according to the reaction

$$Zn_7Sb_2O_{12} + Bi_2O_3(l) \xrightarrow{1050\,°C} Bi_2O_3(Sb, Zn)(l) \quad (8)$$

The liquid phase (l) is originated by reaction between pyrochlore and ZnO described by Equation 1. The temperature range for the reaction between pyrochlore and ZnO agrees with results reported by Inada in a similar system [4].

For the ZBSCCM system (Fig. 2b), evolution of phases is similar to that for the ZBS system, however, the formation of a pyrochlore phase initiates at 800 °C, and reaction between this phase and ZnO occurs in the 950–1100 °C temperature range. Thus, the formation of Bi_2O_3 liquid occurs in a narrower temperature range compared with the ZBS system. As a consequence, a larger amount of liquid phase is present in a narrower temperature range; while in the ZBS system, the formation of Bi_2O_3-rich liquid is gradual. In Fig. 2, in both the ZBS and ZBSCCM systems, the spinel phase starts to form between 800 and 850 °C, before the decomposition reaction of the pyrochlore phase. Considering a Sb_2O_3:Bi_2O_3 ratio equal to two, this spinel phase can be originated by reaction between ZnO and the excess antimony oxide. In Fig. 1 the presence of $ZnSb_2O_6$ is observed at 800 °C. This indicates that this phase could be an intermediate phase in the formation of spinel, since at 900 °C the $ZnSb_2O_6$ phase is not observed by XRD (Fig. 1). In the ZBSCCM system, dissolution of spinel is observed at temperatures higher than 1000 °C.

Thermal analysis in the ZBS system indicates an exothermic reaction at 527 °C, and an endothermic reaction starting at 912 °C and ending at 1071 °C, as observed in the differential curve of Fig. 3. The

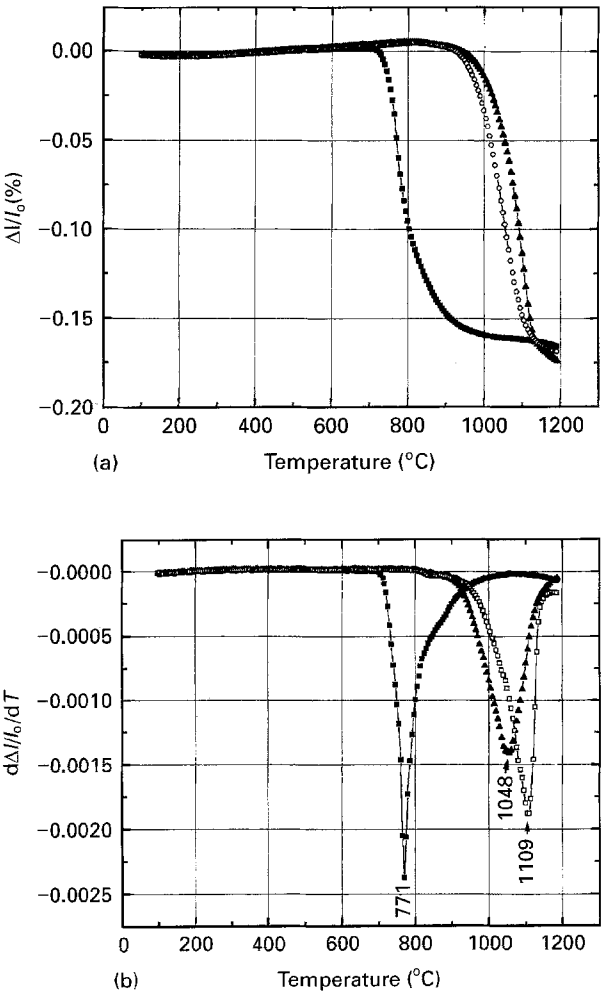

Figure 4 (a) Linear shrinkage, l, as a function of temperature for the (■) ZB, (▲) ZBS and (○) ZBSCCM systems ($\alpha = 10\,^{\circ}C\,min^{-1}$) and (b) Linear shrinkage ratio as a function of temperature for the (■) ZB, (□) ZBS and (▲) ZBSCCM systems ($\alpha = 10\,^{\circ}C\,min^{-1}$).

exothermic reaction is related to the oxidation of Sb_2O_3, since the TGA results show a weight gain of about 1.3 wt % for temperatures higher than 520 °C. This weight gain is close to that theoretically calculated for the oxidation of Sb_2O_3 to Sb_2O_5 (about 1.5 wt %). The endothermic reaction can be related to the reaction between pyrochlore and ZnO, as observed in the HT-XRD results of Fig. 2.

The HT-XRD and TGA–DTA results suggest the following reactions for the ZBS and ZBSCCM systems at the temperature range 600–1100 °C

$$Sb_2O_3(s) + O_2 \xrightarrow{527\,^{\circ}C} Sb_2O_5(l) \quad (9)$$

$$Sb_2O_5(l) + ZnO(s) \xrightarrow{700\text{–}800\,^{\circ}C} ZnSb_2O_6(s) \quad (10)$$

$$ZnSb_2O_6(s) + 6ZnO(s) \xrightarrow{>800\,^{\circ}C} Zn_7Sb_2O_{12}(s) \quad (11)$$

$$3ZnSb_2O_6(s) + 3Bi_2O_3(s) + ZnO(s) \xrightarrow{700 < T < 900\,^{\circ}C} 2Zn_2Bi_3Sb_3O_{14}(s) \quad (12)$$

in addition to Equations 1 and 8.

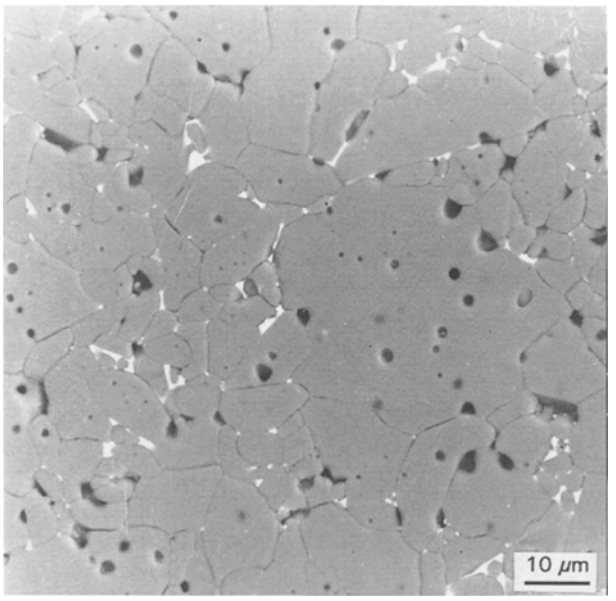

Figure 5 Backscattering SEM micrograph for the ZB system sintered at 1200 °C at a constant heating rate of 10 °C min^{-1}.

3.2. Densification process

Densifications of the ZB, ZBS and ZBSCCM systems were followed by dilatometry for a heating rate of 10 °C min^{-1}, as observed in Fig. 4. Shrinkage of the ZB system starts at 750 °C, reaching a maximum shrinkage rate at 771 °C (Fig. 4b). Fast densification for temperatures above 750 °C is associated with the formation of a bismuth-rich eutectic liquid [7]. The micrograph of Fig. 5 shows a typical microstructure of the ZB system. Two phases, ZnO grains and a Bi_2O_3-rich phase located at triple and quadruple grain boundaries, are observed in this figure. Moreover trapped pores and abnormal grain growth are observed in this figure, which might be due to the fast densification rate promoted by the reactive liquid. When Sb_2O_3 is added to the former system, densification initiates at temperatures above 900 °C; with the maximum shrinkage rate occurring at 1109 °C for the ZBS system and at 1048 °C for the ZBSCCM system, as observed in the Fig. 4.

The pore size distributions for both ZB and ZBS systems are shown in Fig. 6. For the ZB system no reduction of pore volume is observed for sintering temperatures up to 700 °C. However, there is an increase in mean pore size as observed in Fig. 6a. For the sintering temperature of 800 °C, a drastic decrease in the total pore volume is observed, indicating marked densification. Otherwise there is no total pore volume modification for ZBS and ZBSCCM systems for sintering temperatures up to 900 °C. However, the mean pore size increases with sintering temperature in this range.

The shrinkage and pore size distribution results show that the addition of Sb_2O_3 retards the densification process of the ZB system. The liquid formed at 550 °C due to fusion of Sb_2O_5 does not promote any rearrangement or densification in the 550–900 °C range, indicating that this liquid is not reactive with ZnO. The results of HT-XRD indicate that all Bi_2O_3 is consumed by the solid state reaction with $ZnSb_2O_6$

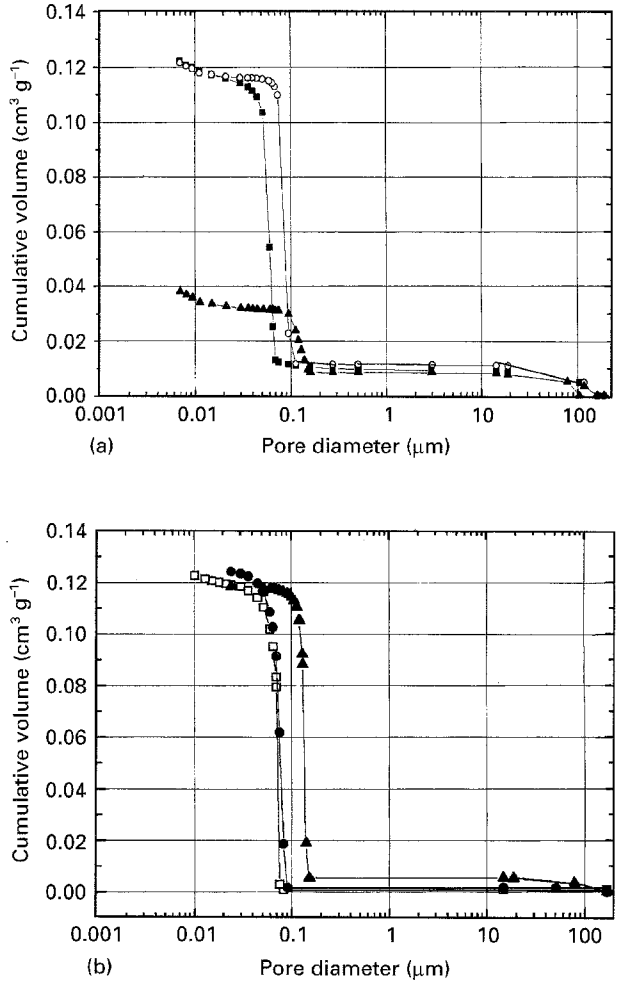

Figure 6 Pore size distribution curve for. (a) ZB system, and (b) ZBS system. (■, □) green, (○, ●) $T = 700\,^{\circ}C$, (▲) $T = 800\,^{\circ}C$ (a) and 900 °C (b).

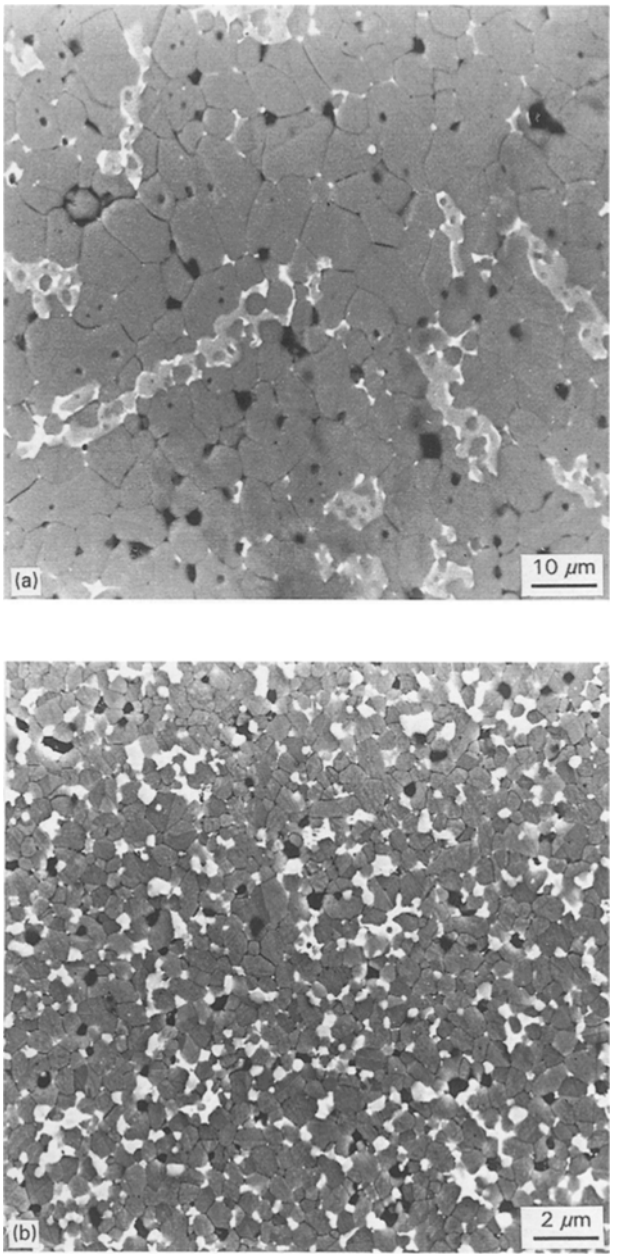

Figure 7 Backscattering SEM micrograph after constant heating rate sintering (5 °C min^{-1}) to 1200 °C for: (a) the ZBS system, and (b) the ZBSCCM system.

and ZnO, forming the pyrochlore phase for $700 < T < 900\,^{\circ}C$, as indicated in Equation 12. This phase reacts with ZnO at temperatures above 950 °C, forming liquid Bi_2O_3. The liquid phase originating from this reaction will promote densification. The formation of a liquid phase above 950 °C is associated with the reaction of ZnO and the pyrochlore phase, as proposed by Kim *et al.* [9] for an Sb_2O_3:Bi_2O_3 ratio greater than one. Additions of transition metals (system ZBSCCM) promote the decomposition reaction of the pyrochlore phase in a narrower temperature range, resulting in densification at a lower temperature.

3.3. Microstructural evolution and grain growth

The addition of Sb_2O_3 markedly alters the phase formation reaction in the ZB system, as well as densification, due to the formation of a reactive liquid at higher temperatures. Then for the ZBS and ZBSCCM systems, one expects greater microstructural modifications.

XRD analysis showed the presence of δ-Bi_2O_3, $Zn_7Sb_2O_{12}$ and ZnO after sintering of the ZBS and ZBSCCM systems. Although the same phases are present for both systems, the micrographs of Fig. 7 show distinct microstructures. Three phases are observed for the ZBS system: ZnO grains, a Bi_2O_3-rich phase and an elongated $Zn_7Sb_2O_{12}$ (SP) phase. These three phases are also observed for the ZBSCCM phase; however, the $Zn_7Sb_2O_{12}$ grains are equiaxial and are homogeneously distributed through the microstructure. In the ZBS system (Fig. 8a), spinel grains are elongated, with size ranging from 15 to 20 μm, and coexist with a Bi_2O_3-rich phase. The spinel grains for the ZBSCCM system are equiaxial, with size ranging from 1 to 2 μm (Fig. 8b). EDS analysis of the spinel grains of this system shows the presence of Zn, Sb, Mn, Cr and Co. Moreover, EDS analysis of several regions of the microstructure indicates that these transition metals locate preferentially in the spinel grains, as reported by Olson *et al.* [13]. Figs 7 and 8 show that the final grain size for the ZBSCCM system is smaller than that of the ZBS system.

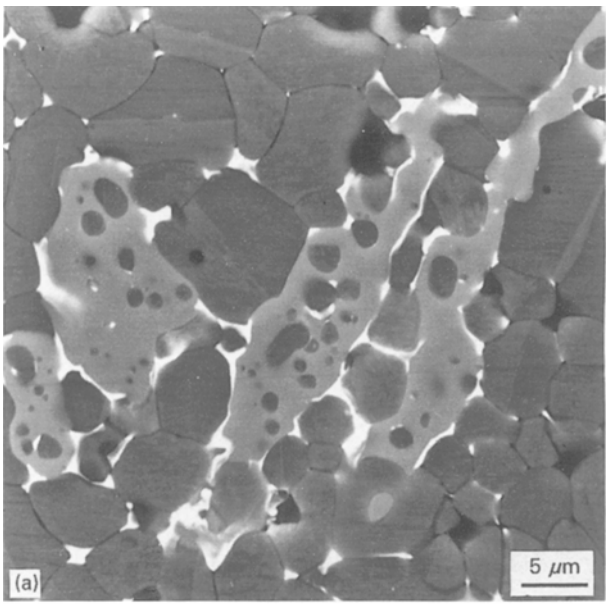

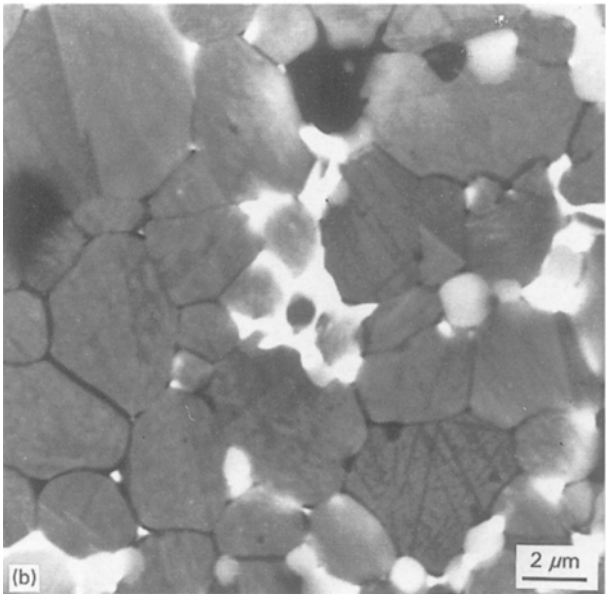

Figure 8 Backscattering SEM micrograph after constant heating rate sintering to 1200 °C for: (a) the ZBS system (2.5 °C min^{-1}), and (b) the ZBSCCM system (5 °C min^{-1}).

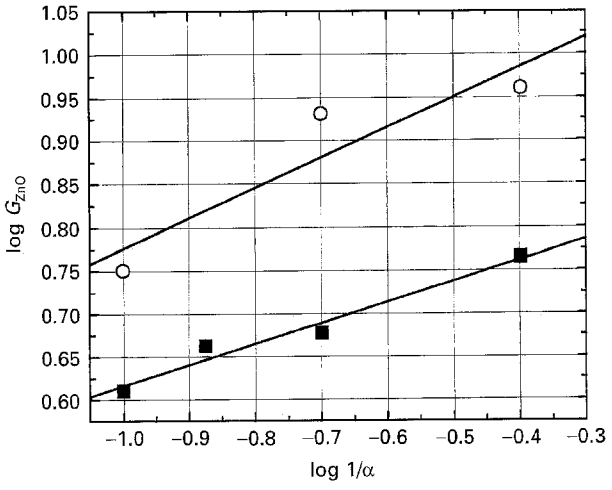

Figure 9 Log plot of ZnO grain size as a function of the reciprocal heating rate for the (○) ZBS and (■) ZBSCCM systems. Final sintering temperature, 1200 °C.

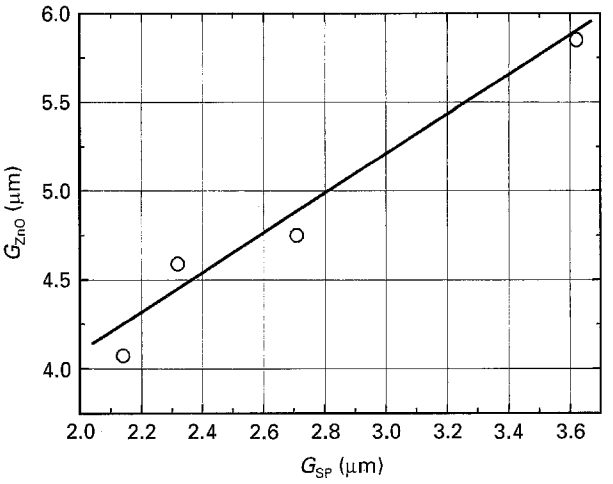

Figure 10 ZnO grain size as a function of spinel grain size after sintering at 1200 °C (ZBSCCM system).

Fig. 9 shows ZnO grain size, G_{ZnO}, as a function of the reciprocal heating rate for both ZBS and ZBSCCM systems. Considering Equation 7, $n = 2.9$ for the ZBS system and $n = 4.2$ for the ZBSCCM system are related. The value $n = 3$ is typical for grain growth kinetics in the presence of a reactive liquid phase [14]. In these cases, the limiting mass transport mechanism for grain growth is normally attributed to solid diffusion in the liquid phase or to the reaction in the solid–liquid interface (Ostwald ripening). In this way, grain growth for the ZBS system can be attributed to the presence of a Bi_2O_3-rich liquid phase, formed from the decomposition of pyrochlore. For the ZBSCCM system, the Bi_2O_3-rich liquid should also promote grain growth. The higher value for n (4.2) for the ZBSCCM system should be related to the smaller observed grain size (Fig. 7). Considering that $dG/d(1/\alpha)$ is proportional to $1/n$, larger n leads to a lower grain growth rate.

The cause for the decrease in the grain growth rate could be related to the morphology and spinel phase distribution in the ZBSCCM system. As shown in Figs 7 and 8, the equiaxial spinel phase is homogeneously distributed in the ZnO grain boundary. That can act as grain boundary pinning, reducing its mobility and as a consequence reducing grain growth [15]. Fig. 10 shows a linear relation between ZnO grain size, G_{ZnO}, and spinel grain size, G_{SP}, resulting that G_{ZnO} is proportional to G_{SP}. According to Zenner's law [16], the second phase acts as pinning when its size G_s, is proportional to the matrix grain size, G_m, i.e.

$$G_m \propto (1/f)\, G_s \qquad (13)$$

where f is the second phase volumetric fraction. Then, based on Zenner's law and on Fig. 10 one can conclude that the spinel phase is acting as a pinning for ZnO grain growth.

Chen and Shen [11] identified a value $n = 6$ for the system containing ZnO, Bi_2O_3, Sb_2O_3, Cr_2O_3, CoO and MnO_2, and ascribed this to the effect of transition metals (CoO, MnO_2 and Cr_2O_3) on zinc vacancies' diffusivities in the ZnO grains, i.e. the effect of

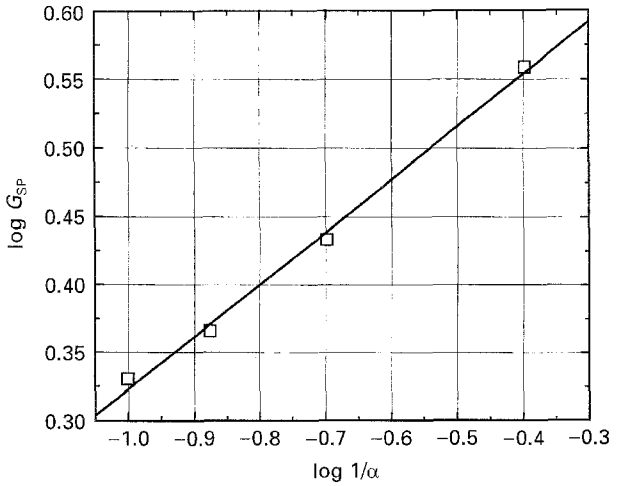

Figure 11 Log plot of spinel grain size as a function of the reciprocal heating rate for the ZBSCCM system. Final sintering temperature, 1200 °C.

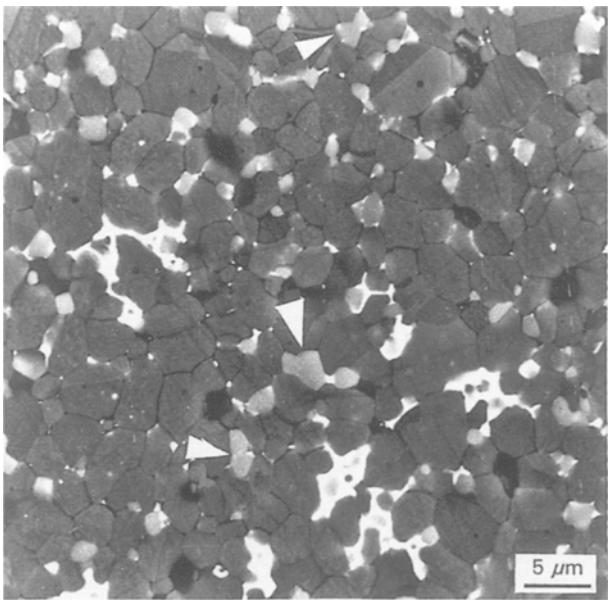

Figure 12 Backscattering SEM micrograph after constant heating rate sintering to 1200 °C (5 °C min^{-1}) of the ZBSCCM system. Arrows indicate spinel grains coalescence.

transition metals is directly related to defects in the ZnO phase. Wu *et al.* [17] observed that an increase in the amount of antimony ions for the ZBSCCM system leads to an increase in the n value from 6 to 8, and as consequence there is a decrease in the ZnO grain growth rate. Increasing the amount of antimony leads to an increase of the spinel phase. This behaviour also suggests that the spinel phase acts as pinning according to Equation 13.

3.4. Spinel ($Zn_7Sb_2O_{12}$) grain growth

Fig. 11 shows the spinel grain size as function of $1/\alpha$ for the ZBSCCM system, with a linear relationship of $n = 2.6$. This value is close to three and can indicate grain growth by the Ostwald ripening mechanism, as suggested by Olson *et al.* [13]. This hypothesis is consistent with the results of HT-XRD, where it is observed that the spinel phase is dissolved at higher temperatures. However, coalescence between spinel grains can also occur due to displacement of the grain boundary during the sintering process. The micrograph of Fig. 12 shows the coalescence process among spinel grains (indicated by arrows).

3.5. General discussion

The addition of Sb_2O_3 to the ZB system, at an Sb_2O_3:Bi_2O_3 equal to two ratio, increases the liquid phase formation temperature due to the formation of a pyrochlore phase; as shown by HT-XRD, dilatometry and mercury porosimetry results. Before formation of the liquid phase, there is no densification in any of the systems studied. However, ZnO with no additives starts densification at temperatures as low as 600 °C, with large densification for temperatures in the range 650–700 °C [8, 18]. In the case of the ZB system, a small fraction of Bi_2O_3 can be dissolved in the ZnO lattice [16]. The dissolved Bi^{3+} ions could segregate in the grain boundary and inhibit the densification process [8]. For the ZBS and ZBSCCM systems, the formation of the pyrochlore phase should inhibit the mass transport for densification and consume the Zn^{2+} ions to form the $Zn_2Bi_3Sb_3O_{14}$ and $ZnSb_2O_6$ phases. Moreover, the pyrochlore phase originates from liquid Sb_2O_5, forming a film on the ZnO particles that inhibits the transport of Zn^{2+} ions. Decomposition of the pyrochlore phase leads to the formation of liquid Bi_2O_3 and $Zn_7Sb_2O_{12}$. The addition of CoO, MnO_2 and Cr_2O_3 to the ZBS system decreases the temperature range for decomposition of the pyrochlore phase, promoting densification at lower temperatures compared with the ZBS system.

Besides their influence on the decomposition temperature of the pyrochlore phase, the transition metal oxides alter significantly the morphology of spinel grains, as illustrated in Figs 7 and 8. In the ZBSCCM system, the spinel phase should act as pinning for grain growth of the ZnO phase and alter the grain growth exponent. In this way the action of CoO, MnO_2 and Cr_2O_3 is to modify the grain morphology of the spinel phase that acts as inclusions for grain growth. Then, these transition metal oxides have an indirect effect on ZnO grain growth, contrary to the direct effect proposed by Chen and Shen [11] and Asokan *et al.* [10].

The equiaxial form of the spinel grains suggests that the dissolved transition metal oxides increase the surface tension of the spinel phase that becomes less wet by the Bi_2O_3-rich liquid.

During spinel grain growth in the ZBSCCM system, two simultaneous mechanisms should act, as illustrated in Fig. 13. Small spinel grains should be dissolved in the Bi_2O_3-rich liquid and be precipitated into large grains (Fig. 13a). Besides this characteristic Ostwald ripening-type mechanism, there is coalescence of spinel grains due to displacement of the grain boundary (Fig. 13b). The Ostwald ripening mechanism should be favoured when the spinel grains are related to the Bi_2O_3-rich liquid, i.e. when they originate from decomposition of the pyrochlore phase.

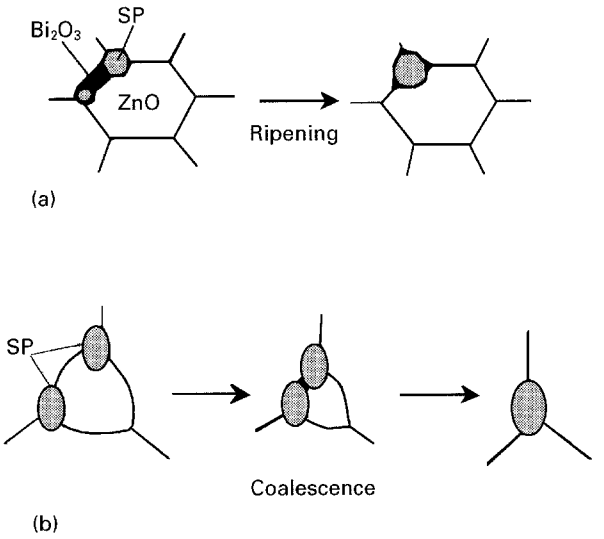

Figure 13 Qualitative model for spinel grain growth: (a) Ostwald ripening, and (b) coalescence.

4. Conclusions

The results of this study lead to the following conclusions.

1. HT-XRD results show that the formation of the pyrochlore phase in the ZBS system initiates at 700 °C and decomposes at 1100 °C. Additions of transition metal oxides (MnO_2, CoO and Cr_2O_3) decrease the temperature range for decomposition of the pyrochlore phase.

2. Formation of the pyrochlore phase inhibits the densification process of ZnO. The decomposition of the pyrochlore phase leads to formation of a Bi_2O_3-rich liquid that promotes liquid phase sintering of ZnO.

3. Additions of transition metal oxides alter the spinel phase morphology to equiaxial grains. These grains act as pinning for grain boundary motion and change the ZnO grain growth kinetics. The grain growth exponent, n, increases from 2.9 for the ZBS system to 4.2 for the ZBSCCM system, showing decrease in the rate of grain growth.

4. The exponent for spinel grain growth kinetics for the ZBSCCM system is $n = 2.6$, and this process is due to two mechanisms: Ostwald ripening and coalescence.

Acknowledgements

The authors acknowledge FINEP/PADCT and CNPq for financial support of this work.

References

1. E. OLSSON and G. L. DUNLOP, *J. Appl. Phys.* **66** (1989) 5072.
2. *Idem, ibid.* **66** (1989) 3666.
3. M. INADA, *Jpn. J. Appl. Phys.* **19** (1980) 409.
4. *Idem, ibid.* **17** (1978) 1.
5. M. INADA and M. MATSUOKA, "Advances in Ceramics", Vol. 7, edited by M. Fyan and A. H. Heuer (The American Ceramic Society, Columbus, OH, 1983) p. 91.
6. J. WONG, *J. Appl. Phys.* **51** (1980) 4453.
7. T. SENDA and R. C. BRADT, *J. Am. Ceram. Soc.* **73** (1990) 106.
8. J. KIM, T. KIMURA and T. YAMAGUCHI, *ibid.* **72** (1989) 1541.
9. *Idem, ibid.* **72** (1989) 1390.
10. T. ASOKAN, G. N. K. IYENGAR and G. R. NAGABHUSHANA, *J. Mater. Sci.* **22** (1987) 2229.
11. Y. C. CHEN and C. Y. SHEN, *J. Appl. Phys.* **69** (1991) 8363.
12. M. I. MENDELSON, *J. Am. Ceram. Soc.* **52** (1969) 443.
13. E. OLSSON, G. DUNLOP and R. OSTERLUND, *ibid.* **76** (1993) 65.
14. K. W. LAY, *ibid.* **51** (1968) 373.
15. J. E. BURKE, in "Sintering Key Papers", edited by S. Somiya and Y. Moriyoshi (Elsevier, London, 1990) p. 39.
16. C. S. SMITH, *Trans. AIME* **175** (1948) 15.
17. L. WU, C. Y. SHEN, Y. C. CHEN, Y. F. WEI, M. H. CHEN and K. C. HUANG, *Jpn. J. Appl. Phys.* **30** (1991) 2850.
18. O. J. WHITTEMORE and J. A. VARELA, *J. Am. Ceram. Soc.* **64** (1981) C154.

Received 9 August 1995
and accepted 18 March 1996